Signal Processing 90 (2010) 784–794

Contents lists available at ScienceDirect

Signal Processing

journal homepage: www.elsevier.com/locate/sigpro

Autocalibration algorithm for mutual coupling of planar array

Chao Liu, Zhongfu Ye *, Yufeng Zhang

Institute of Statistical Signal Processing, Department of Electronic Engineering and Information Science, University of Science and Technology of China (USTC), Hefei, Anhui 230027, PR China

ARTICLE INFO

Article history:
Received 28 November 2008
Received in revised form
13 August 2009
Accepted 14 August 2009
Available online 6 September 2009

Keywords:
Planar array
Uniform hexagon array (UHA)
Mutual coupling
2-D DOA
Autocalibration algorithm

ABSTRACT

With few exceptions, high resolution direction of arrival (DOA) estimation algorithms suffer a lot from the mutual coupling between different array elements. In order to compensate this effect, two autocalibration methods are proposed for the 2-D DOA estimation on a planar array. Both of them can estimate the DOAs without any iterative process or calibration sources. We prove that the effect of mutual coupling can be automatically eliminated by the inherent mechanism of the proposed methods. Moreover, they can also achieve an obvious performance improvement even when there is a coupling model mismatch. After getting the DOA estimations, two methods are proposed to estimate the mutual coupling coefficients. Moreover, these coefficient estimates can be used to further improve the accuracy of DOA estimations. The Cramer–Rao lower bound (CRB) for the parameter estimations are also presented as the benchmark. Simulation results demonstrate the effectiveness of the proposed algorithms.

1. Introduction

In the past decades, the estimation of the direction of arrival (DOA) emitted by narrowband sources has been an active area of research in the signal processing community. High resolution direction finding methods such as MUSIC and ESPRIT have been developed, and theoretical analysis as well as computer simulations have validated their potentially excellent performance [1,2]. Yet despite this potential advantage offered by high resolution methods, their application to real systems has been very limited due to the errors in the array manifold. Especially, the presence of unknown mutual coupling between array elements is known to significantly degrade the performance of most high resolution direction finding algorithms [3–5]. Although it has been proved that known mutual coupling does not affect the estimation performance [6], it is difficult to determine the coupling coefficients as a priori at most of the time.

In order to resolve this issue, many array calibration algorithms have been developed in the past years. The most likely way to obtain information required for calibration is to carry out some measurements, which is usually done by using several calibration sources at known locations [7–10]. However, it may be difficult to set calibration sources in some occasion and the array errors may slowly change with time, so that these methods will be limited in practice. Genetic algorithm is also introduced for mutual coupling calibration due to its good performance of parameter optimization [10]. However, this procedure has the drawback of being time consuming due to the expensive computation. In Ref. [11], impedance matching techniques have been proposed for multiple antenna systems to counteract the effects of mutual coupling. However, the application of this method is limited due to the increase of the complexity of hardware.

Thus, people pay more attention to the autocalibration algorithms in recent years. Some iterative procedures have

* Corresponding author.
E-mail addresses: disneyl@mail.ustc.edu.cn (C. Liu), yezf@ustc.edu.cn (Z. Ye), myth@mail.ustc.edu.cn (Y. Zhang).

0165-1684/$ - see front matter © 2009 Elsevier B.V. All rights reserved.
doi:10.1016/j.sigpro.2009.08.014

been presented to compensate the manifold errors [12–14], but these methods are time consuming due to the large amount of computation. Some other autocalibration algorithms have been proposed in [15–20] without any iterative processes. However, most of these algorithms are based on the uniform linear array (ULA) or the uniform circular array (UCA) and do not deal with the 2-D DOA estimation problem.

There are few researches on 2-D DOA estimation in the presence of mutual coupling. Ref. [21] proposed a hybrid algorithm based on the uniform circular array rank reduction (UCA-RARE) and Root-MUSIC algorithm for 2-D DOA estimation. However, since they exploited a series of Bessel functions to approximate the array manifold, the estimation performance will be affected. Moreover, this method cannot estimate the mutual coupling coefficients. Ref. [22] presented an autocalibration algorithm for 2-D DOA estimation with uniform rectangular array, which can achieve a good performance. However, other planar arrays, such as uniform hexagon array (UHA), are also widely used in practice [23], and algorithms based on these arrays are still need to be studied.

Some other researches have suggested that placing auxiliary elements around the original array can eliminate mutual coupling effect [24–27]. In Ref. [24], the author has analyzed the performance of ESPRIT algorithm with auxiliary elements, and in [26] many auxiliary elements are used to estimate the angles when mutual coupling is significant. Unfortunately, they only verified the validity of the method through experiments without any theoretical explanation on it, and it is hard to find out the way of setting the auxiliary elements from their researches.

A simple coupling model was presented based on the electromagnetic analysis in [28,29], which has been used in many researches. It has been shown that a banded symmetric Toeplitz matrix can be used as model for the mutual coupling. By taking the UHA shown in Fig. 2 as an example of planar array, we extend the mutual coupling model to this array. Then, we propose two autocalibration algorithms for mutual coupling with the UHA in this paper. Afterwards, two estimation methods of mutual coupling coefficients are also proposed by using the DOA estimates. The effect of coupling model mismatch is also analyzed. Furthermore, we can use the estimates of mutual coupling coefficients to further improve the performance of the DOA estimation. Cramer–Rao lower bound (CRB) for planar array in the presence of unknown mutual coupling is also provided as a benchmark of the proposed algorithms. Simulation results demonstrate the effectiveness of the proposed methods.

In this paper, the symbols $(\cdot)^T$, $(\cdot)^H$ and $(\cdot)^\dagger$ denote transpose, conjugate transpose and the Moore–Penrose inverse of the matrix, respectively. The symbols $\odot$ and $\|\cdot\|$ denote the Hadamard product and the Frobenius norm, respectively. The symbols $E\{\cdot\}$, $\mathrm{Re}\{\cdot\}$, $\mathrm{Im}\{\cdot\}$ and $\det\{\cdot\}$ represent the mathematical expectation, take real part, take imaginary part and the matrix determinant, respectively. The symbol $\mathrm{toeplitz}\{\mathbf{v}\}$ denotes the symmetric Toeplitz matrix constructed by the vector $\mathbf{v}$. The symbol $\mathrm{diag}\{z_1,\ldots,z_n\}$ represents a diagonal matrix with diagonal entries $z_1,\ldots,z_n$, and the symbol $\mathrm{diag}\{\mathbf{Z}\}$ represents a vector composed of the main diagonal elements of the matrix $\mathbf{Z}$ as $[\mathbf{Z}_{11},\ldots,\mathbf{Z}_{nn}]^T$. The symbol $\mathrm{blkdiag}\{\mathbf{Z}_1,\ldots,\mathbf{Z}_n\}$ represents a block diagonal matrix with diagonal entries $\mathbf{Z}_1,\ldots,\mathbf{Z}_n$.

2. Array signal model

Consider a planar array composed of N identical isotropic elements, and K ($K<N$) narrowband uncorrelated sources $s_1(t),s_2(t),\ldots,s_K(t)$ impinge on the array from directions $(\theta_1,\varphi_1),(\theta_2,\varphi_2),\ldots,(\theta_K,\varphi_K)$, where θ_i and φ_i denote the azimuth and elevation of the i th source. The azimuth and elevation of the spherical coordinates system are defined in Fig. 1. These far-field sources are assumed to have identical center wavelength λ which is known to the receiver. The additive sensor noises are independent identically distributed (i.i.d.), white Gaussian with common variance σ_n^2.

Assume $\mathbf{C}$ denotes the mutual coupling matrix (MCM) of the planar array. Then the output of the array can be expressed as follows:

$$\mathbf{x}(t)=\mathbf{CAs}(t)+\mathbf{n}(t) \tag{1}$$

where $\mathbf{x}(t)$, $\mathbf{A}$, $\mathbf{s}(t)$ and $\mathbf{n}(t)$ denote the received signal vector, the ideal steering matrix, the source signal vector, and the noise vector, respectively. They are defined as

$$\mathbf{x}(t)=[x_1(t),\ldots,x_N(t)]^T$$
$$\mathbf{A}=[\mathbf{a}(\theta_1,\varphi_1),\ldots,\mathbf{a}(\theta_K,\varphi_K)]$$
$$\mathbf{s}(t)=[s_1(t),\ldots,s_K(t)]^T$$
$$\mathbf{n}(t)=[n_1(t),\ldots,n_N(t)]^T$$

The steering vector can be expressed as $\mathbf{a}(\theta,\varphi)=\exp\{jk\mathbf{r}\upsilon\}$, in which $k=2\pi/\lambda$, $\upsilon=[\cos\theta\cos\varphi,\sin\theta\cos\varphi]^T$ and $\mathbf{r}$ is the coordinates of the array elements defined as $\mathbf{r}=[\mathbf{r}_x,\mathbf{r}_y]$, where $\mathbf{r}_x=[x_1,\ldots,x_N]^T$ is the x-axis vector and $\mathbf{r}_y=[y_1,\ldots,y_N]^T$ is the y-axis vector.

For simplicity, the algorithms proposed in this paper will be discussed mainly based on the UHA shown in Fig. 2. It has been shown in [28,29] that the coupling between two elements with the same interspace is almost the same, and the magnitude of the coupling parameter diminishes quite rapidly along with the increasing of sensor spacing. Generally, mutual coupling coefficients

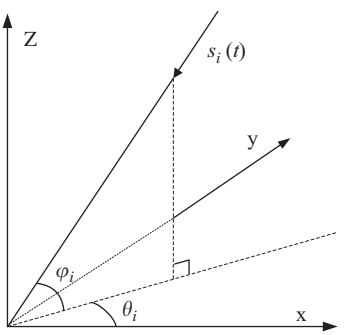

Fig. 1. Definition of azimuth and elevation in the spherical coordinates system.

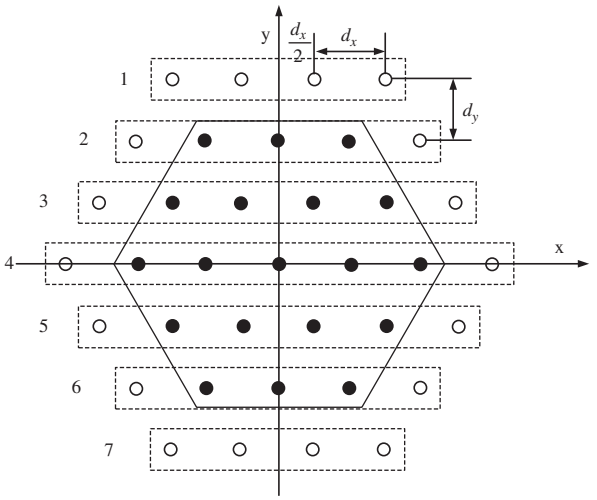

Fig. 2. Geometric configuration of the UHA. The hollow ones represent the elements that would be set as the auxiliary sensors (described in Section 3.2).

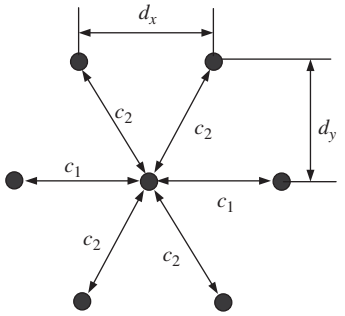

Fig. 3. Sketch map of mutual coupling for UHA. Each sensor is affected by the coupling of the six sensors around it, and this influence descends along with the increasing of the sensor spacing.

between two far apart elements can be approximated to zero, then it is often sufficient to consider the coupling model with just a few nonzero coefficients. In this paper, we assume that one sensor is only affected by the coupling of the six sensors around it, which is shown in Fig. 3. Assume there are P nonzero mutual coupling coefficients embedded in the MCM $\mathbf{C}$ and here $P=3$. Divide the whole UHA into seven linear subarrays, and then the MCM $\mathbf{C}$ can be expressed as

$$\mathbf{C}=\begin{bmatrix} \mathbf{C}_{11} & \mathbf{C}_{12} & \mathbf{0} & \cdots & \mathbf{0} \\ \mathbf{C}_{21} & \mathbf{C}_{22} & \mathbf{C}_{23} & \cdots & \mathbf{0} \\ \vdots & \ddots & \ddots & \ddots & \vdots \\ \mathbf{0} & \cdots & \mathbf{C}_{65} & \mathbf{C}_{66} & \mathbf{C}_{67} \\ \mathbf{0} & \cdots & \mathbf{0} & \mathbf{C}_{76} & \mathbf{C}_{77} \end{bmatrix}_{N\times N} \tag{2}$$

where the submatrices $\mathbf{C}_{ii}$ are the MCMs of the i th subarray and $\mathbf{C}_{ij}$ are the MCMs between the i th and the j th linear subarray with the size $N_i\times N_j$, and they are defined as

$$\mathbf{C}_{ii}=\text{toeplitz}\{[1,c_1,0,\ldots,0]_{1\times N_i}\}$$

$$\mathbf{C}_{ij}=\begin{cases}\mathbf{C}_i & N_j=N_i+1\\ \mathbf{C}_i^T & N_j=N_i-1\end{cases} \tag{3}$$

and

$$\mathbf{C}_i=\begin{bmatrix} c_2 & c_2 & 0 & \cdots & 0 \\ 0 & c_2 & c_2 & \cdots & 0 \\ \vdots & \ddots & \ddots & \ddots & \vdots \\ 0 & \cdots & 0 & c_2 & c_2 \end{bmatrix} \tag{4}$$

where N_i is the element number of the i th subarray with $\sum_{i=1}^{7}N_i=N$ shown in Fig. 2, and $\mathbf{C}_{ji}=\mathbf{C}_{ij}^T$.

The covariance matrix of the received signal vector is

$$\mathbf{R_x}=E\{\mathbf{x}(t)\mathbf{x}^H(t)\}=\mathbf{CAR_sA}^H\mathbf{C}^H+\sigma_n^2\mathbf{I}_N \tag{5}$$

in which $\mathbf{R_s}$ is the source covariance matrix, and $\mathbf{I}_N$ is the $N\times N$ identity matrix.

By performing eigen-decomposition of $\mathbf{R_x}$, we can obtain

$$\mathbf{R_x}=\sum_{i=1}^{K}\lambda_i\boldsymbol{e}_i\boldsymbol{e}_i^H+\sum_{i=K+1}^{N}\lambda_i\boldsymbol{e}_i\boldsymbol{e}_i^H=\mathbf{E_s}\mathbf{\Lambda_s}\mathbf{E_s}^H+\sigma^2\mathbf{E_n}\mathbf{E_n}^H \tag{6}$$

in which $\lambda_1\geq\lambda_2\geq\cdots\geq\lambda_K>\lambda_{K+1}=\cdots=\lambda_N=\sigma_n^2$ are the eigenvalues of $\mathbf{R_x}$ and $\boldsymbol{e}_1,\boldsymbol{e}_2,\ldots,\boldsymbol{e}_N$ are their associated eigenvectors. The columns of $\mathbf{E_s}$ and $\mathbf{E_n}$ are the eigenvectors associated with the K largest eigenvalues and $N-K$ smallest eigenvalues, respectively. The number of the far-field sources K can be estimated by the minimum description length (MDL) principle [30]. For simplicity, we assume that the number of signals is known in this paper.

3. DOA estimation and mutual coupling calibration

3.1. DOA estimation for planar array: method 1

Friedlander and Weiss gave a useful transformation about mutual coupling for ULA and UCA in [12], and many calibration algorithms have been developed based on this transformation. However, mutual coupling in planar array is rarely mentioned. Here, we will give a similar transformation for the UHA and use it to estimate the DOAs. Sorting the elements by the subarrays from left to right and from top to bottom (as shown in Fig. 2), then the steering vector can be rewritten as

$$\mathbf{a}(\theta,\varphi)=[\beta_1\mathbf{a}_4^T,\beta_2\mathbf{a}_5^T,\beta_3\mathbf{a}_6^T,\beta_4\mathbf{a}_7^T,\beta_5\mathbf{a}_6^T,\beta_6\mathbf{a}_5^T,\beta_7\mathbf{a}_4^T]^T \tag{7}$$

$$\beta_i=\exp\{jk[x_{i1}\cos\theta\cos\varphi+y_{i1}\sin\theta\cos\varphi]\},\quad i=1,\ldots,7 \tag{8}$$

in which $x_{i1}=(6-|4-i|)d_x/2$ and $y_{i1}=(4-i)d_y$ are the coordinates of the first element of the i th linear subarray, and

$$\mathbf{a}_i=[1,\beta,\ldots,\beta^{i-1}]^T \tag{9}$$

where $\beta=\exp\{jkd_x\cos\theta\cos\varphi\}$. Then, from (2) and (7) we have

$$\mathbf{Ca}=\begin{bmatrix}\mathbf{C}_{11}&\mathbf{C}_{12}&\mathbf{0}&\cdots&\mathbf{0}\\ \mathbf{C}_{21}&\mathbf{C}_{22}&\mathbf{C}_{23}&\cdots&\mathbf{0}\\ \vdots&\ddots&\ddots&\ddots&\vdots\\ \mathbf{0}&\cdots&\mathbf{C}_{65}&\mathbf{C}_{66}&\mathbf{C}_{67}\\ \mathbf{0}&\cdots&\mathbf{0}&\mathbf{C}_{76}&\mathbf{C}_{77}\end{bmatrix}\begin{bmatrix}\beta_1\mathbf{a}_4\\ \beta_2\mathbf{a}_5\\ \vdots\\ \beta_6\mathbf{a}_5\\ \beta_7\mathbf{a}_4\end{bmatrix}$$
$$=\begin{bmatrix}\beta_1\mathbf{C}_{11}\mathbf{a}_4+\beta_2\mathbf{C}_{12}\mathbf{a}_5\\ \beta_1\mathbf{C}_{21}\mathbf{a}_4+\beta_2\mathbf{C}_{22}\mathbf{a}_5+\beta_3\mathbf{C}_{23}\mathbf{a}_6\\ \vdots\\ \beta_5\mathbf{C}_{65}\mathbf{a}_6+\beta_6\mathbf{C}_{66}\mathbf{a}_5+\beta_7\mathbf{C}_{67}\mathbf{a}_4\\ \beta_6\mathbf{C}_{76}\mathbf{a}_5+\beta_7\mathbf{C}_{77}\mathbf{a}_4\end{bmatrix} \tag{10}$$

Consequently, we have

$$\mathbf{C}_{ii}\mathbf{a}_{N_i}=\mathbf{T}_{ii}[1,c_1]^T,\quad \mathbf{C}_{ij}\mathbf{a}_{N_j}=\mathbf{T}_{ij}c_2 \tag{11}$$

The $N_i\times 2$ matrix $\mathbf{T}_{ii}$ can be given by the sum of the two $N_i\times 2$ following matrices [12]:

$$\mathbf{T}_{i1}(m,n)=\begin{cases}\mathbf{a}_{N_i}(m+n-1), & m+n\le N_i+1\\ 0 & \text{otherwise}\end{cases}$$
$$\mathbf{T}_{i2}(m,n)=\begin{cases}\mathbf{a}_{N_i}(m-n+1), & m\le n\le 2\\ 0 & \text{otherwise}\end{cases} \tag{12}$$

and $\mathbf{T}_{ij}$ are $N_i\times 1$ vectors given as follows:

$$\mathbf{T}_{ij}=\begin{cases}(1+\beta)\mathbf{a}_{N_j-1}, & N_j=N_i+1\\ ([0,\mathbf{a}_{N_j}^T]^T+[\mathbf{a}_{N_j}^T,0]^T), & N_j=N_i-1\end{cases} \tag{13}$$

Then, (10) can be rewritten as

$$\mathbf{Ca}=\mathbf{Tc} \tag{14}$$

where $\mathbf{c}=[1,c_1,c_2]^T$ and

$$\mathbf{T}=\begin{bmatrix}\mathbf{T}_{11}&\mathbf{T}_{12}\\ \mathbf{T}_{22}&\mathbf{T}_{21}+\mathbf{T}_{23}\\ \vdots&\vdots\\ \mathbf{T}_{66}&\mathbf{T}_{65}+\mathbf{T}_{67}\\ \mathbf{T}_{77}&\mathbf{T}_{76}\end{bmatrix}_{N\times 3} \tag{15}$$

Since the columns of $\mathbf{E_s}$ span the column space of $\mathbf{CA}$, while those of $\mathbf{E_n}$ span its orthogonal space, then we have [6]

$$\|\mathbf{E}_\mathbf{n}^H\mathbf{Ca}(\theta_i,\varphi_i)\|=0\quad \text{for} i=1,\ldots,K \tag{16}$$

Substituting (14) into (16), we have

$$\mathbf{E}_\mathbf{n}^H\mathbf{T}(\theta_i,\varphi_i)\mathbf{c}=\mathbf{0} \tag{17}$$

When $N-K\ge 2$, the above homogeneous linear equation with respect to $\mathbf{c}$ has only one linear independent solution, and the $(N-K)\times 3$ matrix $\mathbf{E}_\mathbf{n}^H\mathbf{T}(\theta_i,\varphi_i)$ is rank one defect. Define the matrix $\mathbf{Q}(\theta,\varphi)=\mathbf{T}^H(\theta,\varphi)\mathbf{E_n}\mathbf{E}_\mathbf{n}^H\mathbf{T}(\theta,\varphi)$, then $\mathbf{Q}$ is full rank unless $(\theta,\varphi)=(\theta_i,\varphi_i)$ (proof in Appendix A). Therefore, we can construct the following spatial spectrum to estimate the DOAs:

$$P(\theta,\varphi)=\frac{1}{\det(\mathbf{Q}(\theta,\varphi))} \tag{18}$$

For a more general situation, there is also a similar relationship with (14) for an arbitrary planar array. Assume there are P nonzero mutual coupling coefficients embedded in the MCM $\mathbf{C}$, and $\mathbf{c}=[1,c_1,\ldots,c_{P-1}]^T$, then we have a similar relationship with the above

$$\mathbf{Ca}=\mathbf{Tc} \tag{19}$$

Similarly define the matrix $\mathbf{Q}(\theta,\varphi)=\mathbf{T}^H(\theta,\varphi)\mathbf{E_n}\mathbf{E}_\mathbf{n}^H\mathbf{T}(\theta,\varphi)$, and then (18) can be used to estimate the DOAs (proof in Appendix A).

3.2. DOA estimation for planar array: method 2

In order to eliminate the effect of the mutual coupling, we set the sensors on the boundary of the UHA as auxiliary sensors (hollow ones shown in Fig. 2). And then, the output of the middle subarray can be expressed as

$$\tilde{\mathbf{x}}(t)=\mathbf{Px}(t)=\mathbf{PCAs}(t)+\mathbf{Pn}(t) \tag{20}$$

where $\tilde{\mathbf{x}}(t)=[x_{M_1+2}(t),\ldots,x_{M_2-1}(t),\ldots,x_{M_5+2}(t),\ldots,x_{M_6-1}(t)]^T$, $M_j=\sum_{i=1}^{j}N_i$, and the $\tilde{N}\times N$ matrix $\mathbf{P}$ is defined as

$$\mathbf{P}=[\mathbf{O},\mathbf{J},\mathbf{O}],\quad \mathbf{J}=\text{blkdiag}\{\mathbf{J}_2,\mathbf{J}_3,\mathbf{J}_4,\mathbf{J}_5,\mathbf{J}_6\} \tag{21}$$

where $\tilde{N}=\sum_{i=2}^{6}(N_i-2)$ is the number of the middle subarray (composed of solid elements shown in Fig. 2), $\mathbf{O}$ is a $\tilde{N}\times N_1$ zero matrix and

$$\mathbf{J}_i=\begin{bmatrix}0&1&0&\cdots&0\\ \vdots&\ddots&\ddots&\ddots&\vdots\\ 0&\cdots&0&1&0\end{bmatrix}_{(N_i-2)\times N_i},\quad i=2,\ldots,6$$

Consequently, we have

$$\mathbf{Pn}(t)=\tilde{\mathbf{n}}(t),\quad \mathbf{PC}=\tilde{\mathbf{C}} \tag{22}$$

Then the output of the middle subarray can be rewritten as

$$\tilde{\mathbf{x}}(t)=\tilde{\mathbf{C}}\mathbf{As}(t)+\tilde{\mathbf{n}}(t) \tag{23}$$

where $\tilde{\mathbf{n}}(t)=[n_{M_1+2}(t),\ldots,n_{M_2-1}(t),\ldots,n_{M_5+2}(t),\ldots,n_{M_6-1}(t)]^T$, and the MCM $\tilde{\mathbf{C}}$ in (23) can be expressed as

$$\tilde{\mathbf{C}}=\begin{bmatrix}\tilde{\mathbf{C}}_{21}&\tilde{\mathbf{C}}_{22}&\tilde{\mathbf{C}}_{23}&\cdots&\mathbf{0}\\ \vdots&\ddots&\ddots&\ddots&\vdots\\ \mathbf{0}&\cdots&\tilde{\mathbf{C}}_{65}&\tilde{\mathbf{C}}_{66}&\tilde{\mathbf{C}}_{67}\end{bmatrix} \tag{24}$$

where $\tilde{\mathbf{C}}_{ij}$ are submatrices of $\tilde{\mathbf{C}}$ defined as

$$\tilde{\mathbf{C}}_{ij}=\mathbf{J}_i\mathbf{C}_{ij},\quad i=2,\ldots,6 \tag{25}$$

Therefore, the covariance matrix of the received signals can be given by

$$\tilde{\mathbf{R}}_\mathbf{x}=E\{\tilde{\mathbf{x}}(t)\tilde{\mathbf{x}}^H(t)\}=\tilde{\mathbf{C}}\mathbf{AR_sA}^H\tilde{\mathbf{C}}^H+\sigma^2\mathbf{I}_{\tilde{N}} \tag{26}$$

where $\mathbf{I}_{\tilde{N}}$ is the $\tilde{N}\times\tilde{N}$ identity matrix. Through the eigen-decomposition process of $\tilde{\mathbf{R}}_\mathbf{x}$, we can get the signal subspace spanned by $\tilde{\mathbf{E}}_\mathbf{s}$ and noise subspace spanned by $\tilde{\mathbf{E}}_\mathbf{n}$ of the middle UHA. Similar with (16), we have the following equation for the middle subarray:

$$\|\tilde{\mathbf{E}}_\mathbf{n}^H\tilde{\mathbf{C}}\mathbf{a}(\theta_i,\varphi_i)\|=0\quad \text{for} i=1,\ldots,K \tag{27}$$

According to the characteristic of $\tilde{\mathbf{C}}$, we have a very important relationship as follows:

$$\tilde{\mathbf{C}}\mathbf{a} = \begin{bmatrix} \tilde{\mathbf{C}}_{21} & \tilde{\mathbf{C}}_{22} & \tilde{\mathbf{C}}_{23} & \cdots & \mathbf{0} \\ \vdots & \ddots & \ddots & \ddots & \vdots \\ \mathbf{0} & \cdots & \tilde{\mathbf{C}}_{65} & \tilde{\mathbf{C}}_{66} & \tilde{\mathbf{C}}_{67} \end{bmatrix} \begin{bmatrix} \beta_1\mathbf{a}_4 \\ \vdots \\ \beta_7\mathbf{a}_4 \end{bmatrix} = \begin{bmatrix} \beta_1\tilde{\mathbf{C}}_{21}\mathbf{a}_4 + \beta_2\tilde{\mathbf{C}}_{22}\mathbf{a}_5 + \beta_3\tilde{\mathbf{C}}_{23}\mathbf{a}_6 \\ \vdots \\ \beta_5\tilde{\mathbf{C}}_{65}\mathbf{a}_6 + \beta_6\tilde{\mathbf{C}}_{66}\mathbf{a}_5 + \beta_7\tilde{\mathbf{C}}_{67}\mathbf{a}_4 \end{bmatrix} \tag{28}$$

According to the structure of $\tilde{\mathbf{C}}_{ij}$, we have the following relationship:

$$\tilde{\mathbf{C}}_{ij}\mathbf{a}_{N_j} = \begin{cases} (c_1 + \beta + c_1\beta^2)\mathbf{a}_{N_j-2}, & N_j = N_i \\ c_2(1+\beta)\mathbf{a}_{N_j-1}, & N_j = N_i - 1 \\ c_2\beta(1+\beta)\mathbf{a}_{N_j-3}, & N_j = N_i + 1 \end{cases} \tag{29}$$

Substitute (29) into (28), and use the notation $\beta_y = \exp\{jkd_y\sin\theta\cos\varphi\}$, $\beta = \exp\{jkd_x\cos\theta\cos\varphi\}$, we have

$$\begin{aligned} \tilde{\mathbf{C}}\mathbf{a} &= \begin{bmatrix} [\beta_1 c_2(1+\beta) + \beta_2(c_1+\beta+c_1\beta^2) + \beta_3 c_2\beta(1+\beta)]\mathbf{a}_3 \\ \vdots \\ [\beta_5 c_2\beta(1+\beta) + \beta_6(c_1+\beta+c_1\beta^2) + \beta_7 c_2(1+\beta)]\mathbf{a}_3 \end{bmatrix} \\ &= \begin{bmatrix} \tilde{\beta}_2[\beta^{-1/2}\beta_y(1+\beta)c_2 + (\beta^{-1}c_1 + 1 + c_1\beta) + \beta^{-1/2}\beta_y^{-1}(1+\beta)c_2]\mathbf{a}_3 \\ \vdots \\ \tilde{\beta}_6[\beta^{-1/2}\beta_y(1+\beta)c_2 + (\beta^{-1}c_1 + 1 + c_1\beta) + \beta^{-1/2}\beta_y^{-1}(1+\beta)c_2]\mathbf{a}_3 \end{bmatrix} \\ &= c(\theta,\varphi)[\tilde{\beta}_2\mathbf{a}_3^T, \tilde{\beta}_3\mathbf{a}_4^T, \tilde{\beta}_4\mathbf{a}_5^T, \tilde{\beta}_5\mathbf{a}_4^T, \tilde{\beta}_6\mathbf{a}_3^T]^T \\ &= c(\theta,\varphi)\tilde{\mathbf{a}}(\theta,\varphi) \end{aligned} \tag{30}$$

where

$$\begin{aligned} c(\theta,\varphi) &= \beta^{-1/2}\beta_y(1+\beta)c_2 + (\beta^{-1}c_1 + 1 + c_1\beta) \\ &\quad + \beta^{-1/2}\beta_y^{-1}(1+\beta)c_2 \\ &= 1 + 2\cos(kd_x\cos\theta\cos\varphi)c_1 \\ &\quad + 4\cos(kd_x\cos\theta\cos\varphi/2)\cos(kd_y\sin\theta\cos\varphi)c_2 \end{aligned} \tag{31}$$

$$\tilde{\mathbf{a}}(\theta,\varphi) = [\tilde{\beta}_2\mathbf{a}_3^T, \tilde{\beta}_3\mathbf{a}_4^T, \tilde{\beta}_4\mathbf{a}_5^T, \tilde{\beta}_5\mathbf{a}_4^T, \tilde{\beta}_6\mathbf{a}_3^T]^T \tag{32}$$

$$\tilde{\beta}_i = \exp\{jk[x_{i2}\cos\theta\cos\varphi + y_{i2}\sin\theta\cos\varphi]\}, \quad i = 2,\ldots,6 \tag{33}$$

where $x_{i2} = (4 - |4-i|)d_x/2$ and $y_{i2} = (4-i)d_y$ are the coordinates of the second element in the i th subarray, and $\mathbf{a}_i$ has been defined in (9). Obviously, $\tilde{\mathbf{a}}(\theta,\varphi)$ is the steering vector of the middle subarray. Since $c(\theta,\varphi)$ is a scalar, it does not affect the orthogonality between $\tilde{\mathbf{a}}$ and $\tilde{\mathbf{E}}_\mathbf{n}$. Then, from (30) and (27), we have

$$\|\tilde{\mathbf{E}}_\mathbf{n}^H\tilde{\mathbf{a}}(\theta_i,\varphi_i)\| = 0 \quad \text{for} i = 1,\ldots,K \tag{34}$$

By using the relationship displayed in (34), the following spatial spectrum can be used to estimate the DOAs

$$P_m(\theta,\varphi) = \frac{1}{\|\tilde{\mathbf{E}}_\mathbf{n}^H\tilde{\mathbf{a}}(\theta,\varphi)\|^2} \tag{35}$$

3.3. Mutual coupling estimation and autocalibration

After obtaining the DOA estimates via the methods proposed in Sections 3.1 and 3.2, we can further estimate the mutual coupling coefficients by utilizing the signals received from all sensors (including auxiliary sensors on the boundary). Form (17) we can obtain

$$\sum_{i=1}^{K}\mathbf{T}^H(\theta_i,\varphi_i)\mathbf{E}_\mathbf{n}\mathbf{E}_\mathbf{n}^H\mathbf{T}(\theta_i,\varphi_i)\mathbf{c} = \mathbf{Z}_c\mathbf{c} = \mathbf{0} \tag{36}$$

$$\mathbf{Z}_c = \sum_{i=1}^{K}\mathbf{T}^H(\theta_i,\varphi_i)\mathbf{E}_\mathbf{n}\mathbf{E}_\mathbf{n}^H\mathbf{T}(\theta_i,\varphi_i) \tag{37}$$

Obviously, the vector $\mathbf{c}$ lies in the null space of the matrix $\mathbf{Z}_c$. Since the above homogeneous linear equations with respect to $\mathbf{c}$ have only one linear independent solution, the null space of $\mathbf{Z}_c$ is one-dimensional (proof in Appendix A). Assume $\boldsymbol{e}_{\min}$ is the eigenvector of $\mathbf{Z}_c$ associated with the minimal eigenvalue, the coupling coefficients can be obtained by

$$\mathbf{c} = \boldsymbol{e}_{\min}/\boldsymbol{e}_{\min}(1) \tag{38}$$

Since the nonnegativity of Frobenius norm, using Eq. (17), the coupling coefficients can be obtained by the following constraint quadratic optimization problem

$$\mathbf{c} = \arg\min_{\mathbf{c}}\sum_{i=1}^{K}\|\mathbf{E}_\mathbf{n}^H\mathbf{T}(\theta_i,\varphi_i)\mathbf{c}\|^2 \quad \text{s.t. } \mathbf{w}^H\mathbf{c} = 1 \tag{39}$$

The above optimization problem can be rewritten as

$$\mathbf{c} = \arg\min_{\mathbf{c}}\mathbf{c}^H\mathbf{Z}_c\mathbf{c} \quad \text{s.t. } \mathbf{w}^H\mathbf{c} = 1 \tag{40}$$

where $\mathbf{w} = [1,0,\ldots,0]^T$. Then the result can be obtained by the method of Lagrange multipliers

$$\mathbf{c} = \frac{\mathbf{Z}_c^\dagger\mathbf{w}}{\mathbf{w}^H\mathbf{Z}_c^\dagger\mathbf{w}} \tag{41}$$

Once the coupling coefficient vector $\mathbf{c}$ is determined, we can reconstruct the MCM $\mathbf{C}$ and use it to refine the DOA estimation by using the full array with the following spectrum function:

$$P_M(\theta,\varphi) = \frac{1}{\|\mathbf{E}_n^H\mathbf{C}\mathbf{a}(\theta,\varphi)\|^2} \tag{42}$$

3.4. Algorithm summary and model mismatch analysis

In order to make the procedure of the proposed algorithms clearer, we give a summary as follows

1. Use the array output data to estimate the covariance matrices

$$\hat{\mathbf{R}}_\mathbf{x} = \frac{1}{L}\sum_{i=1}^{L}\mathbf{x}(i)\mathbf{x}^H(i) \tag{43}$$

$$\hat{\tilde{\mathbf{R}}}_\mathbf{x} = \frac{1}{L}\sum_{i=1}^{L}\tilde{\mathbf{x}}(i)\tilde{\mathbf{x}}^H(i) \tag{44}$$

   where L is the number of snapshots.
2. Get their respective noise subspaces $\hat{\mathbf{E}}_\mathbf{n}$ and $\hat{\tilde{\mathbf{E}}}_\mathbf{n}$;
3. Use $\hat{\mathbf{E}}_\mathbf{n}$ and (18) (method 1) or $\hat{\tilde{\mathbf{E}}}_\mathbf{n}$ and (35) (method 2) to get the initial estimates of the DOAs.
4. Use the initial estimates of the DOAs and the coupling estimation method in (38) or (41) to estimate the mutual coupling coefficients and then reconstruct the MCM $\hat{\mathbf{C}}$.

5. Refine the DOA estimates through (42) by using $\hat{\mathbf{C}}$.
6. Repeat (4) and (5) to further improve the estimation accuracy if needed.

Actually, the two methods presented in Sections 3.1 and 3.2 (step 3) are two individual algorithms to eliminate the effect of mutual coupling, and the following steps are used to improve the estimation performance. Practically, the estimation accuracy of the above algorithm without step 6 can meet the requirement at most of the time. Considering the computational complexity, we do not carry out step 6 in the following simulations.

The above algorithms are based on the coupling model shown in Fig. 3. However, the circumstance of mutual coupling in practice may be more complicated. Here, the performance of the above algorithms will be analyzed when there is a model mismatch of mutual coupling. Assume each sensor in the array is affected by the coupling of the 18 sensors around it as shown in Fig. 4. However, we still use the coupling model shown in Fig. 3 in methods 1 and 2.

Based on the coupling model shown in Fig. 4, the MCM of the whole UHA can be written as

$$\overline{\mathbf{C}} = \begin{bmatrix} \overline{\mathbf{C}}_{11} & \overline{\mathbf{C}}_{12} & \overline{\mathbf{C}}_{13} & \cdots & \mathbf{0} \\ \overline{\mathbf{C}}_{21} & \overline{\mathbf{C}}_{22} & \overline{\mathbf{C}}_{23} & \overline{\mathbf{C}}_{24} & \mathbf{0} \\ \vdots & \ddots & \ddots & \ddots & \vdots \\ \mathbf{0} & \overline{\mathbf{C}}_{64} & \overline{\mathbf{C}}_{65} & \overline{\mathbf{C}}_{66} & \overline{\mathbf{C}}_{67} \\ \mathbf{0} & \cdots & \overline{\mathbf{C}}_{75} & \overline{\mathbf{C}}_{76} & \overline{\mathbf{C}}_{77} \end{bmatrix} = \mathbf{C} + \Delta\mathbf{C} \tag{45}$$

where $\mathbf{C}$ is defined in (2) and $\Delta\mathbf{C} = \mathbf{F}(c_3, c_4, c_5, c_6)$ is the residual mutual coupling matrix which is neglected. As we have proved before that the effect caused by $\mathbf{C}$ has been eliminated, the performance of the proposed methods are mainly affected by $\Delta\mathbf{C}$. Since mutual coupling effect decreases rapidly along with the increasing of the sensor spacing, $|c_3|, |c_4|, |c_5|, |c_6| \ll 1$. Then we have

$$\|\Delta\mathbf{C}\| \ll \|\overline{\mathbf{C}}\| \tag{46}$$

Therefore, although there is a mismatch between the presumed coupling model and actual one, through the above calibration methods, most of the mutual coupling effect can be eliminated except for a small residual impact.

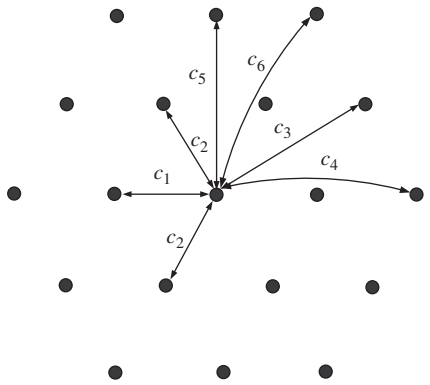

Fig. 4. Sketch map of mutual coupling for UHA. Each sensor is affected by the coupling of the 18 sensors around it. Mutual coupling coefficients between two sensors with the same interspace are the same, and this influence descends along with the increasing of the sensor spacing.

4. Simulations

In this section, the performance of the proposed estimation methods are validated through some simulation examples with the array shown in Fig. 2. Assume the array interspaces are $d_x = d_y = \lambda/2$, where λ is the wavelength of the actual narrowband signals. Since the interspace between two neighboring elements along the oblique direction is larger than that along the horizontal direction, the coupling coefficients c_1 and c_2 should satisfy the relationship $|c_1| > |c_2|$. Considering this fact, we assume the mutual coupling coefficients to be $c_1 = 0.3065 + 0.3951j$, $c_2 = 0.1018 - 0.1721j$. The additive sensor noises are i.i.d., white Gaussian random processes with common variance σ_n^2. Suppose the Gaussian signals are of equal power σ^2, then the input SNR can be defined as $10\log_{10}(\sigma^2/\sigma_n^2)$.

Consider seven independent signals from far-field impinging on the array from $(28.3^\circ, 45.2^\circ)$, $(54.5^\circ, 65.3^\circ)$, $(58.2^\circ, 28.1^\circ)$, $(94.7^\circ, 48.7^\circ)$, $(120.1^\circ, 70.8^\circ)$, $(132.6^\circ, 32.9^\circ)$, $(156.4^\circ, 52.5^\circ)$, which denote the azimuths and elevations of the signals, respectively. The spectrum search area is $[0^\circ, 180^\circ] \times [0^\circ, 90^\circ]$ with the step size of 0.1°.

In the following simulations, 100 Monte Carlo trials are carried out for each experiment to demonstrate the statistical efficiency of the methods proposed in Section 3. The DOA estimation accuracy is measured by the root mean squared error (RMSE) defined as

$$RMSE_{\mathbf{\Theta}} = \sqrt{\left(\sum_{l=1}^{100}\sum_{i=1}^{K} \|\hat{\mathbf{\Theta}}_{il} - \mathbf{\Theta}_i\|^2\right)/(100K)} \tag{47}$$

where $\hat{\mathbf{\Theta}}_{il} = [\hat{\theta}_{il}, \hat{\varphi}_{il}]^T$ is the estimation of $\mathbf{\Theta}_i = [\theta_i, \varphi_i]^T$ in the l th Monte Carlo experiment, and K is the number of sources. Since the values of mutual coupling coefficients are small, we define the relative RMSE to demonstrate the statistical efficiency of the proposed methods as follows:

$$RMSE_{\mathbf{c}} = \sqrt{\left(\sum_{l=1}^{100} \|\hat{\mathbf{c}}_l' - \mathbf{c}'\|^2/\|\mathbf{c}'\|^2\right)/100 \times 100\%} \tag{48}$$

where $\hat{\mathbf{c}}_l'$ is the estimation of $\mathbf{c}' = [c_1, c_2]^T$ in the l th Monte Carlo experiment.

The methods proposed in Sections 3.1 (marked as 'method 1') and 3.2 (marked as 'method 2') are compared with the standard MUSIC algorithm in the presence of unknown mutual coupling. The CRB with unknown mutual coupling is also presented (computed as shown in Appendix B). The RMSE of the DOA estimations versus the SNR and snapshots are shown in Figs. 5 and 6. Since the performance of method 2 is better than that of method 1, the estimation results of method 2 are used to estimate the mutual coupling coefficients by using the methods proposed in Section 3.3. The RMSE of the coupling estimations versus the SNR and snapshots are shown in Figs. 7 and 8. At last, the result of mutual coupling estimations by using (41) is used to further improve the performance of the DOA estimations by using

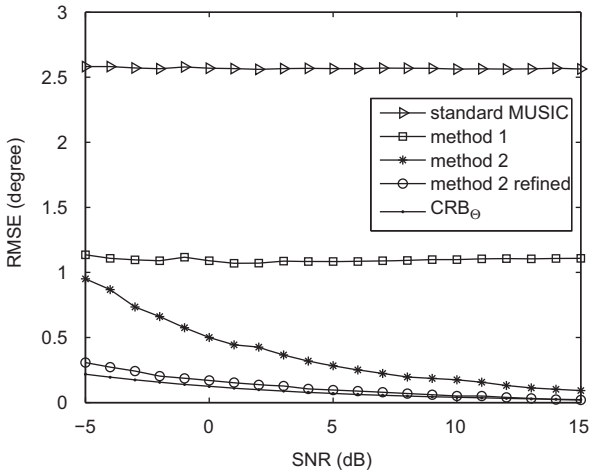

Fig. 5. Performance curve of DOA estimation: RMSE of DOA versus SNR with $L = 500$.

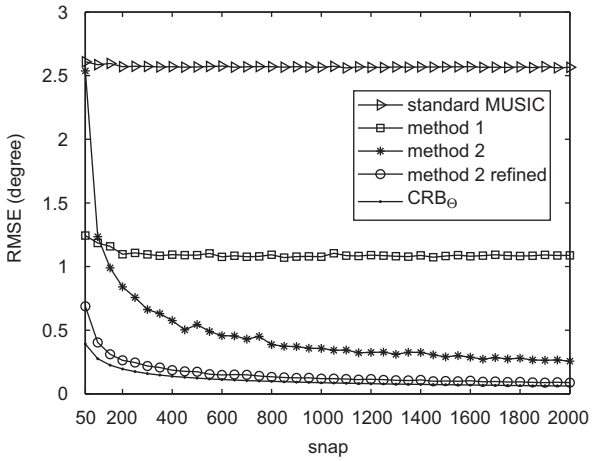

Fig. 6. Performance curve of DOA estimation: RMSE of DOA versus snapshots with SNR = 0 dB.

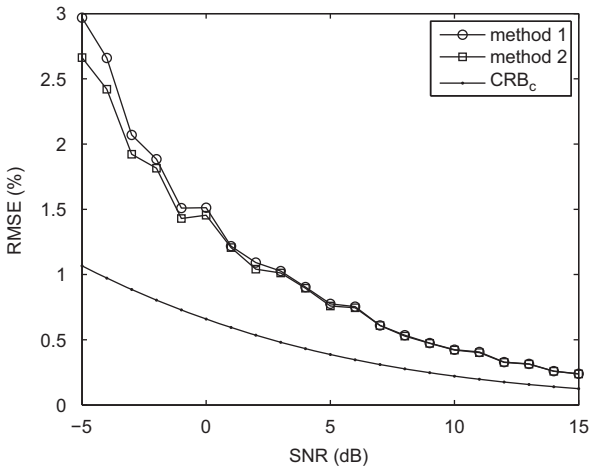

Fig. 7. Performance curve of coupling estimation: RMSE of coupling coefficients versus SNR with $L = 500$.

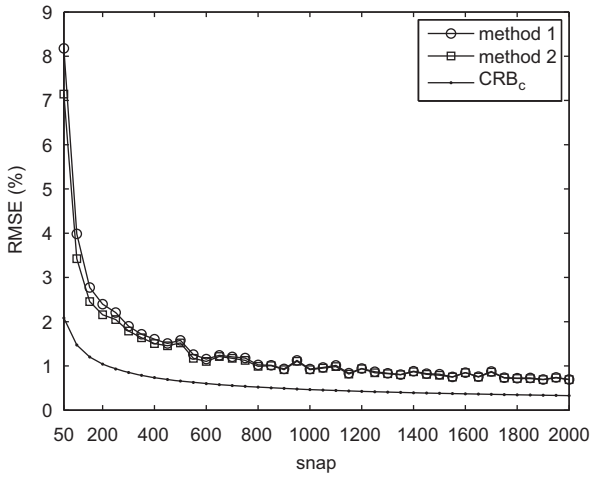

Fig. 8. Performance curve of coupling estimation: RMSE of coupling coefficients versus snapshots with SNR = 0 dB.

(42). The performance is also shown in Figs. 5 and 6, which is marked as 'method 2 refined'.

From Figs. 5 and 6, we can see that each of the proposed methods has an obvious performance improvement over the standard MUSIC algorithm. Although method 1 can be applied to any planar array, its performance is not so good as that of method 2, especially with high SNR. Despite the fact that the position of the spatial spectrum peaks in (18) and (35) are the same as that of (42) (known mutual coupling) theoretically, the value near the peaks may still has effect on estimation result. In (18), this effect is the gain of the ignored function $c(\theta, \varphi)$. At most of the time, this is a slowly varying function, which makes the spectrum in (35) and (42) nearly the same. However, the spectrum in (18) does not have this character. The mutual coupling still has some residual effect on it, which does not change with SNR or snapshots. This caused the estimation error unchanged with SNR or snapshots. By comparison, method 2 has a better performance than method 1 in this condition. However, this method needs a special symmetry of the array geometric configuration. Anyway, each of the two methods can be refined by using the estimates of the mutual coupling to achieve a much better performance that can approach the CRB. As shown in Figs. 7 and 8, each of the two mutual coupling estimation methods has a satisfactory performance and is almost the same as each other.

In the following simulations, the performance of the proposed methods are validated when there is a coupling model mismatch between the presumed (shown in Fig. 3) and the actual one (shown in Fig. 4). Since mutual coupling effect decreases along with the increasing of the sensor spacing [28], we have $1 > |c_1| > |c_2| > |c_3| > |c_4| = |c_5| > |c_6|$. As the proposed methods have little to do with the value of the mutual coupling coefficients, these coefficients are assumed to be $c_1 = 0.3065 + 0.3951j$, $c_2 = 0.1018 - 0.1721j$, $c_3 = -0.0429 + 0.0675j$, $c_4 = c_5 = 0.0405 - 0.0294j$, $c_6 = 0.0093 + 0.0285j$ without loss of generality. The other experimental conditions are the same as the above.

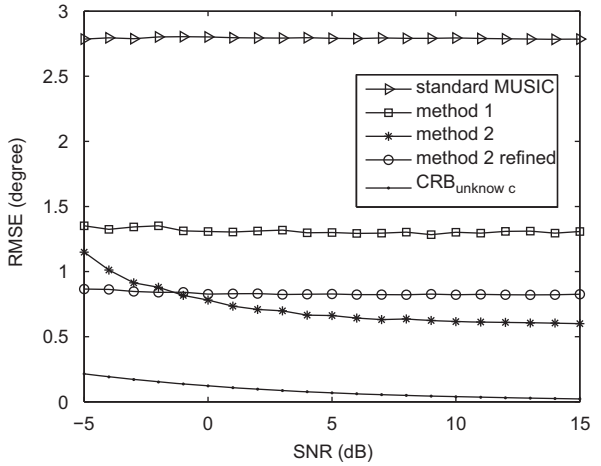

Fig. 9. Performance curve of DOA estimation: RMSE of DOA versus SNR with $L = 500$.

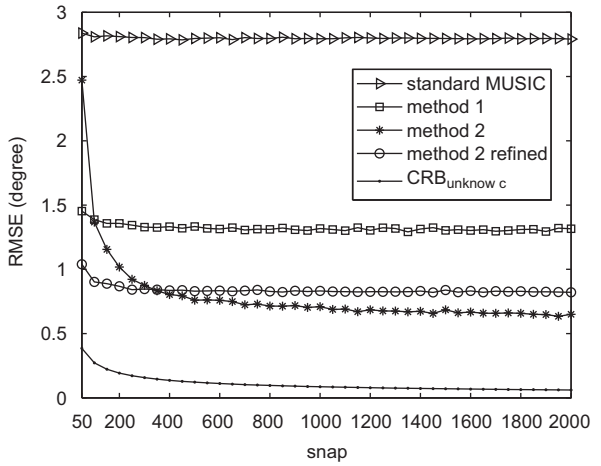

Fig. 10. Performance curve of DOA estimation: RMSE of DOA versus snapshots with SNR = 0 dB.

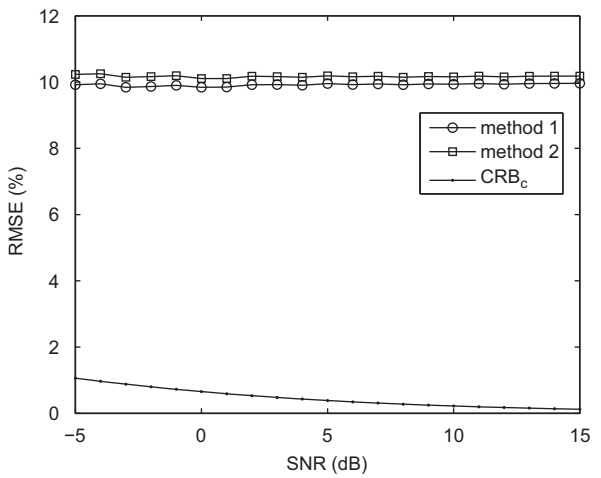

Fig. 11. Performance curve of coupling estimation: RMSE of coupling coefficients versus SNR with $L = 500$.

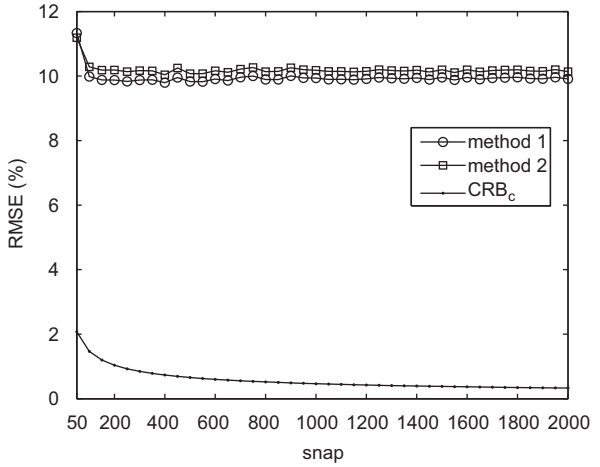

Fig. 12. Performance curve of coupling estimation: RMSE of coupling coefficients versus snapshots with SNR = 0 dB.

The RMSEs versus SNR and number of snapshots are shown in Figs. 9–12. From Figs. 9 and 10 we can see that the proposed methods can still improve the DOA estimation accuracy a lot. However, since several small coefficients are ignored in the proposed methods, the RMSE of the coupling coefficients becomes more significant as shown in Figs. 11 and 12. Therefore, the method proposed in Section 3.3, which is based on the estimated coupling coefficients, even performs worse than method 2. And because of the residual mutual coupling effect, the DOA estimation performance almost does not improve with the increase of SNR or snapshots. However, it can still give a performance improvement over method 2 in low SNR and small snapshots condition.

5. Conclusion

In this paper, we have studied the problem of 2-D DOA estimation for planar array especially for the UHA with unknown mutual coupling. Two autocalibration methods are proposed to deal with this problem. The first method can be applied to arrays with any geometric structure. However, it may have some residual effect of mutual coupling and does not give an excellent performance. By setting the sensors on the boundary of the array as auxiliary sensors, the second method can provide a better performance than the first method. However, this method needs a special symmetry of the array geometric configuration. After getting the estimates of the DOAs, we can estimate the mutual coupling coefficients. This result can be used to further improve the DOA estimation accuracy, which can approach the CRB especially with high SNR. When there is a model mismatch, the proposed methods can still eliminate most of the mutual coupling effect and provide a good performance. Simulation results support the analysis in this paper and demonstrate the effectiveness of our methods.

Appendix A. Proof of rank defect

Assume there are P nonzero mutual coupling coefficients embedded in the MCM $\mathbf{C}$, and $\mathbf{c}=[1,c_1,\ldots,c_{P-1}]^T$, then

$$\mathbf{Ca}=\begin{bmatrix} c_{11} & \cdots & c_{1N} \\ \vdots & & \vdots \\ c_{N1} & \cdots & c_{NN} \end{bmatrix}\begin{bmatrix} a_1 \\ \vdots \\ a_N \end{bmatrix}=\begin{bmatrix} \sum_{i=1}^{N} c_{1i}a_i \\ \vdots \\ \sum_{i=1}^{N} c_{Ni}a_i \end{bmatrix} \tag{A.1}$$

where $c_{ij}\in\{1,c_1,\ldots,c_{P-1},0\}$ and the above equation can be expressed as

$$\mathbf{Ca}=\begin{bmatrix} f_{11}(\mathbf{a})+f_{12}(\mathbf{a})c_1+\cdots+f_{1P}(\mathbf{a})c_{P-1} \\ \vdots \\ f_{11}(\mathbf{a})+f_{N2}(\mathbf{a})c_1+\cdots+f_{NP}(\mathbf{a})c_{P-1} \end{bmatrix}=\mathbf{Tc} \tag{A.2}$$

in which

$$\mathbf{T}=\begin{bmatrix} f_{11}(\mathbf{a}) & \cdots & f_{1P}(\mathbf{a}) \\ \vdots & & \vdots \\ f_{N1}(\mathbf{a}) & \cdots & f_{NP}(\mathbf{a}) \end{bmatrix}_{N\times P} \tag{A.3}$$

where the linear functions f_{ij} relate to the structure of the planar array. Then we have

$$\mathbf{E}_{\mathbf{n}}^H\mathbf{T}(\theta_i,\varphi_i)\mathbf{c}=\mathbf{0},\quad i=1,\ldots,K \tag{A.4}$$

where $\mathbf{E}_{\mathbf{n}}^H\mathbf{T}(\theta_i,\varphi_i)$ is an $(N-K)\times P$ matrix and $N-K\geq(P-1)$.

Assume there are more than one linear independent nonzero solutions of the above homogeneous linear equation with respect to $\mathbf{c}$. Without loss of generality, assume there are two linear independent solutions $\mathbf{c}_0$ and $\mathbf{c}_0'$. By normalizing the first element of them to unity, they can be expressed as

$$\mathbf{c}_0=[1,c_1,\ldots,c_{P-1}]^T\mathbf{c}_0'=[1,c_1',\ldots,c_{P-1}']^T \tag{A.5}$$

Then we have

$$\mathbf{E}_{\mathbf{n}}^H\mathbf{T}(\theta_i,\varphi_i)(\mathbf{c}_0-\mathbf{c}_0')=\mathbf{0} \tag{A.6}$$

Define a new mutual coupling vector $\mathbf{c}_0''=\mathbf{c}_0-\mathbf{c}_0'$. Since $\mathbf{c}_0$ and $\mathbf{c}_0'$ are linear independent, $\mathbf{c}_0''\neq\mathbf{0}$. Obviously, $\mathbf{c}_0''$ is also a solution of (A.4), and

$$\mathbf{c}_0''=[0,(c_1-c_1'),\ldots,(c_{P-1}-c_{P-1}')]^T \tag{A.7}$$

We can see that there are at most $P-1$ nonzero elements in $\mathbf{c}_0''$, which is in contradiction with the above assumption (there are P nonzero mutual coupling coefficients). This contradiction can only be caused by the assumption that there are more than one linear independent solutions of Eq. (A.4). So (A.4) has only one linear independent solution, which coincides with the real mutual coupling coefficients. Based on the subspace theory, the null space of $\mathbf{E}_{\mathbf{n}}^H\mathbf{T}(\theta_i,\varphi_i)$ is one-dimensional.

When $(\theta,\varphi)\neq(\theta_i,\varphi_i)$,

$$\mathbf{E}_{\mathbf{n}}^H\mathbf{T}(\theta,\varphi)\mathbf{c}=\mathbf{x} \tag{A.8}$$

where $\mathbf{x}\neq\mathbf{0}$. Define a new matrix as $\mathbf{B}=\mathbf{E}_{\mathbf{n}}^H\mathbf{T}(\theta,\varphi)=[\mathbf{b}_1,\ldots,\mathbf{b}_P]$. Then, the nonhomogeneous linear equation can be simplified as the following homogeneous linear equation:

$$[\mathbf{b}_1-\mathbf{x},\ldots,\mathbf{b}_P]\mathbf{c}=\mathbf{0} \tag{A.9}$$

Similar with the above process, it can be proved that (A.8) has only one solution. Then the matrix $\mathbf{E}_{\mathbf{n}}^H\mathbf{T}(\theta,\varphi)$ must be full column rank. Define a new matrix as

$$\mathbf{Q}(\theta,\varphi)=\mathbf{T}^H(\theta,\varphi)\mathbf{E}_{\mathbf{n}}\mathbf{E}_{\mathbf{n}}^H\mathbf{T}(\theta,\varphi) \tag{A.10}$$

Since $\mathbf{Q}(\theta,\varphi)$ has the same rank as $\mathbf{E}_{\mathbf{n}}^H\mathbf{T}(\theta,\varphi)$, the matrix $\mathbf{Q}(\theta,\varphi)$ is rank one defect when $(\theta,\varphi)=(\theta_i,\varphi_i)$, and is full rank when $(\theta,\varphi)\neq(\theta_i,\varphi_i)$. Define another matrix as

$$\mathbf{Z}_c=\sum_{i=1}^{K}\mathbf{T}^H(\theta_i,\varphi_i)\mathbf{E}_{\mathbf{n}}\mathbf{E}_{\mathbf{n}}^H\mathbf{T}(\theta_i,\varphi_i) \tag{A.11}$$

Through a similar analysis with the above, we can come to the conclusion that $\mathbf{Z}_c$ is also rank one defect.

Appendix B. Cramer–Rao lower bound for Gaussian signals of planar array

Consider the vector $\mathbf{x}(t)$ as a complex Gaussian vector with zero mean. Then its covariance matrix is

$$\mathbf{C}_{\mathbf{x}}=\mathbf{R}_{\mathbf{x}}=E\{\mathbf{x}(t)\mathbf{x}^H(t)\}=\overline{\mathbf{A}}\mathbf{R}_{\mathbf{s}}\overline{\mathbf{A}}^H+\sigma^2\mathbf{I} \tag{B.1}$$

where $\overline{\mathbf{A}}=\mathbf{CA}$. Define the unknown parameter vector embedded in $\mathbf{R}_{\mathbf{x}}$ as

$$\boldsymbol{\eta}=[\boldsymbol{\theta}^T,\boldsymbol{\varphi}^T,\boldsymbol{a}^T,\boldsymbol{b}^T]^T \tag{B.2}$$

where $\boldsymbol{\theta}=[\theta_1,\ldots,\theta_K]^T$, $\boldsymbol{\varphi}=[\varphi_1,\ldots,\varphi_K]^T$, $\boldsymbol{a}=\mathrm{Re}\{\mathbf{c}'\}$, $\boldsymbol{b}=\mathrm{Im}\{\mathbf{c}'\}$, in which $\mathbf{c}'=[c_1,\ldots,c_{P-1}]^T$.

Assume the number of snapshots is L, then the general expression of the Fisher information matrix (FIM) for Gaussian signals can be given as [12]

$$\mathbf{F}_{mn}=L\,\mathrm{tr}\left\{\mathbf{R}_{\mathbf{x}}^{-1}\frac{\partial\mathbf{R}_{\mathbf{x}}}{\partial\boldsymbol{\eta}_m}\mathbf{R}_{\mathbf{x}}^{-1}\frac{\partial\mathbf{R}_{\mathbf{x}}}{\partial\boldsymbol{\eta}_n}\right\} \tag{B.3}$$

And in the following part, we will give a more detailed expression of the FIM for the problem we proposed above.

B.1. The FIM with respect to the DOAs

In the subsequent derivation process, we define the following notation:

$$\dot{\overline{\mathbf{A}}}_{\boldsymbol{\eta}_m}\triangleq\partial\overline{\mathbf{A}}/\partial\boldsymbol{\eta}_m \tag{B.4}$$

Then, the partial derivative of the covariance matrix can be expressed as

$$\frac{\partial\mathbf{R}_{\mathbf{x}}}{\partial\theta_m}=\dot{\overline{\mathbf{A}}}_{\theta_m}\mathbf{R}_{\mathbf{s}}\overline{\mathbf{A}}^H+\overline{\mathbf{A}}\mathbf{R}_{\mathbf{s}}\dot{\overline{\mathbf{A}}}_{\theta_m}^H \tag{B.5}$$

Since $\mathrm{tr}\{\mathbf{A}+\mathbf{A}^H\}=2\,\mathrm{Re}\{\mathrm{tr}\{\mathbf{A}\}\}$, substituting (B.5) into (B.3), then we have

$$\begin{aligned}\mathbf{F}_{\theta_m\theta_n}=2L\,\mathrm{Re}\{&\mathrm{tr}\{\mathbf{R}_{\mathbf{x}}^{-1}\dot{\overline{\mathbf{A}}}_{\theta_m}\mathbf{R}_{\mathbf{s}}\overline{\mathbf{A}}^H\mathbf{R}_{\mathbf{x}}^{-1}\dot{\overline{\mathbf{A}}}_{\theta_n}\mathbf{R}_{\mathbf{s}}\overline{\mathbf{A}}^H\}\\&+\mathrm{tr}\{\mathbf{R}_{\mathbf{x}}^{-1}\dot{\overline{\mathbf{A}}}_{\theta_m}\mathbf{R}_{\mathbf{s}}\overline{\mathbf{A}}^H\mathbf{R}_{\mathbf{x}}^{-1}\overline{\mathbf{A}}\mathbf{R}_{\mathbf{s}}\dot{\overline{\mathbf{A}}}_{\theta_n}^H\}\}\end{aligned} \tag{B.6}$$

where $\mathbf{A}(\theta,\varphi)=[\exp\{jk\mathbf{r}\upsilon_1\},\ldots,\exp\{jk\mathbf{r}\upsilon_K\}]$, $k=2\pi/\lambda$, $\upsilon_m=[\cos\theta_m\cos\varphi_m,\sin\theta_m\cos\varphi_m]^T$, $\mathbf{r}$ is the coordinates of the array elements defined as $\mathbf{r}=[\mathbf{r}_x,\mathbf{r}_y]$, where $\mathbf{r}_x=[x_1,\ldots,x_N]^T$ is the x-axis vector and $\mathbf{r}_y=[y_1,\ldots,y_N]^T$ is the y-axis vector. Using the definitions given above, then

we have

$$\dot{\mathbf{A}}_{\theta_m} = \left[0,\ldots,jk\exp\{jk\mathbf{r}\upsilon_m\}\odot\left(\mathbf{r}\frac{\partial\upsilon_m}{\partial\theta_m}\right),\ldots,0\right] \tag{B.7}$$

where $\partial\upsilon_m/\partial\theta_m = [-\sin\theta_m\cos\varphi_m, \cos\theta_m\cos\varphi_m]^T$. Note that $\dot{\overline{\mathbf{A}}}_{\theta_m}$ has nonzero value only in the i th column, then it can be written as

$$\dot{\overline{\mathbf{A}}}_{\theta_m} = \mathbf{C}\dot{\mathbf{A}}_{\boldsymbol{\theta}}\boldsymbol{e}_m\boldsymbol{e}_m^T \tag{B.8}$$

where the select vector $\boldsymbol{e}_m$ is the m th column of $\mathbf{I}_{K\times K}$ and $\dot{\mathbf{A}}_{\boldsymbol{\theta}}$ is the matrix of derivatives given by

$$\dot{\mathbf{A}}_{\boldsymbol{\theta}} = \left[jk\exp\{jk\mathbf{r}\upsilon_1\}\odot\left(\mathbf{r}\frac{\partial\upsilon_1}{\partial\theta_1}\right),\ldots,jk\exp\{jk\mathbf{r}\upsilon_K\}\odot\left(\mathbf{r}\frac{\partial\upsilon_K}{\partial\theta_K}\right)\right] \tag{B.9}$$

Use the notation

$$\dot{\overline{\mathbf{A}}}_{\boldsymbol{\theta}} \triangleq \mathbf{C}\dot{\mathbf{A}}_{\boldsymbol{\theta}} \tag{B.10}$$

and then (B.6) becomes

$$\begin{aligned}\mathbf{F}_{\theta_m\theta_n} &= 2L\,\mathrm{Re}\{\mathrm{tr}\{\mathbf{R}_{\mathbf{x}}^{-1}\dot{\overline{\mathbf{A}}}_{\boldsymbol{\theta}}\boldsymbol{e}_m\boldsymbol{e}_m^T\mathbf{R}_{\mathbf{s}}\overline{\mathbf{A}}^H\mathbf{R}_{\mathbf{x}}^{-1}\dot{\overline{\mathbf{A}}}_{\boldsymbol{\theta}}\boldsymbol{e}_n\boldsymbol{e}_n^T\mathbf{R}_{\mathbf{s}}\overline{\mathbf{A}}^H\}\\ &\quad+\mathrm{tr}\{\mathbf{R}_{\mathbf{x}}^{-1}\dot{\overline{\mathbf{A}}}_{\boldsymbol{\theta}}\boldsymbol{e}_m\boldsymbol{e}_m^T\mathbf{R}_{\mathbf{s}}\overline{\mathbf{A}}^H\mathbf{R}_{\mathbf{x}}^{-1}\overline{\mathbf{A}}\mathbf{R}_{\mathbf{s}}\boldsymbol{e}_n\boldsymbol{e}_n^T\dot{\overline{\mathbf{A}}}_{\boldsymbol{\theta}}^H\}\}\\ &= 2L\,\mathrm{Re}\{\boldsymbol{e}_m^T\mathbf{R}_{\mathbf{s}}\overline{\mathbf{A}}^H\mathbf{R}_{\mathbf{x}}^{-1}\dot{\overline{\mathbf{A}}}_{\boldsymbol{\theta}}\boldsymbol{e}_n\boldsymbol{e}_n^T\mathbf{R}_{\mathbf{s}}\overline{\mathbf{A}}^H\mathbf{R}_{\mathbf{x}}^{-1}\dot{\overline{\mathbf{A}}}_{\boldsymbol{\theta}}\boldsymbol{e}_m\\ &\quad+\boldsymbol{e}_m^T\mathbf{R}_{\mathbf{s}}\overline{\mathbf{A}}^H\mathbf{R}_{\mathbf{x}}^{-1}\overline{\mathbf{A}}\mathbf{R}_{\mathbf{s}}\boldsymbol{e}_n\boldsymbol{e}_n^T\dot{\overline{\mathbf{A}}}_{\boldsymbol{\theta}}^H\mathbf{R}_{\mathbf{x}}^{-1}\dot{\overline{\mathbf{A}}}_{\boldsymbol{\theta}}\boldsymbol{e}_m\}\end{aligned} \tag{B.11}$$

Therefore

$$\begin{aligned}\mathbf{F}_{\theta\theta} &= 2L\,\mathrm{Re}\{(\mathbf{R}_{\mathbf{s}}\overline{\mathbf{A}}^H\mathbf{R}_{\mathbf{x}}^{-1}\dot{\overline{\mathbf{A}}}_{\boldsymbol{\theta}})\\ &\quad\odot(\mathbf{R}_{\mathbf{s}}\overline{\mathbf{A}}^H\mathbf{R}_{\mathbf{x}}^{-1}\dot{\overline{\mathbf{A}}}_{\boldsymbol{\theta}})^T+(\mathbf{R}_{\mathbf{s}}\overline{\mathbf{A}}^H\mathbf{R}_{\mathbf{x}}^{-1}\overline{\mathbf{A}}\mathbf{R}_{\mathbf{s}})\\ &\quad\odot(\dot{\overline{\mathbf{A}}}_{\boldsymbol{\theta}}^H\mathbf{R}_{\mathbf{x}}^{-1}\dot{\overline{\mathbf{A}}}_{\boldsymbol{\theta}})^T\}\end{aligned} \tag{B.12}$$

Similarly define

$$\dot{\mathbf{A}}_{\boldsymbol{\varphi}} = \left[jk\exp\{jk\mathbf{r}\upsilon_1\}\odot\left(\mathbf{r}\frac{\partial\upsilon_1}{\partial\varphi_1}\right),\ldots,jk\exp\{jk\mathbf{r}\upsilon_K\}\odot\left(\mathbf{r}\frac{\partial\upsilon_K}{\partial\varphi_K}\right)\right] \tag{B.13}$$

where $\partial\upsilon_m/\partial\varphi_m = [-\cos\theta_m\sin\varphi_m, -\sin\theta_m\sin\varphi_m]^T$, and then we can get $\mathbf{F}_{\boldsymbol{\varphi\varphi}}$, $\mathbf{F}_{\boldsymbol{\varphi\theta}}$ and $\mathbf{F}_{\boldsymbol{\theta\varphi}}$ like the above.

B.2. The FIM with respect to mutual coupling parameters

From (14) we have

$$\dot{\overline{\mathbf{A}}}_{a_m} = \frac{\partial\mathbf{C}}{\partial a_m}\mathbf{A} = [\mathbf{T}(\theta_1,\varphi_1)\boldsymbol{e}_{m+1},\ldots,\mathbf{T}(\theta_K,\varphi_K)\boldsymbol{e}_{m+1}],\quad m=1,\ldots,P-1 \tag{B.14}$$

where the select vector $\boldsymbol{e}_m$ is the m th column of $\mathbf{I}_{P\times P}$. Replacing θ_m,θ_n in (B.6) by the parameters of mutual coefficients a_m,a_n, we can get

$$\begin{aligned}\mathbf{F}_{a_ma_n} &= 2L\,\mathrm{Re}\{\mathrm{tr}\{\mathbf{R}_{\mathbf{x}}^{-1}\dot{\overline{\mathbf{A}}}_{a_m}\mathbf{R}_{\mathbf{s}}\overline{\mathbf{A}}^H\mathbf{R}_{\mathbf{x}}^{-1}\dot{\overline{\mathbf{A}}}_{a_n}\mathbf{R}_{\mathbf{s}}\overline{\mathbf{A}}^H\}\\ &\quad+\mathrm{tr}\{\mathbf{R}_{\mathbf{x}}^{-1}\dot{\overline{\mathbf{A}}}_{a_m}\mathbf{R}_{\mathbf{s}}\overline{\mathbf{A}}^H\mathbf{R}_{\mathbf{x}}^{-1}\overline{\mathbf{A}}\mathbf{R}_{\mathbf{s}}\dot{\overline{\mathbf{A}}}_{a_n}^H\}\}\end{aligned} \tag{B.15}$$

Replacing θ_m,θ_n in (B.6) by other parameters of mutual coefficients, and we can similarly get other elements of FIM such as $\mathbf{F}_{b_mb_n}$, $\mathbf{F}_{a_mb_n}$ and $\mathbf{F}_{b_ma_n}$.

B.3. The FIM with respect to DOA-coupling cross terms

Similar with the process above, we can obtain

$$\begin{aligned}\mathbf{F}_{\theta_ma_n} &= 2L\,\mathrm{Re}\{\boldsymbol{e}_m^T\mathbf{R}_{\mathbf{s}}\overline{\mathbf{A}}^H\mathbf{R}_{\mathbf{x}}^{-1}\dot{\overline{\mathbf{A}}}_{a_n}\mathbf{R}_{\mathbf{s}}\overline{\mathbf{A}}^H\mathbf{R}_{\mathbf{x}}^{-1}\dot{\overline{\mathbf{A}}}_{\boldsymbol{\theta}}\boldsymbol{e}_m\\ &\quad+\boldsymbol{e}_m^T\mathbf{R}_{\mathbf{s}}\overline{\mathbf{A}}^H\mathbf{R}_{\mathbf{x}}^{-1}\overline{\mathbf{A}}\mathbf{R}_{\mathbf{s}}\dot{\overline{\mathbf{A}}}_{a_n}^H\mathbf{R}_{\mathbf{x}}^{-1}\dot{\overline{\mathbf{A}}}_{\boldsymbol{\theta}}\boldsymbol{e}_m\}\end{aligned} \tag{B.16}$$

and then we have

$$\begin{aligned}\mathbf{F}_{\boldsymbol{\theta}a_n} &= 2L\,\mathrm{Re}\{\mathrm{diag}\{\mathbf{R}_{\mathbf{s}}\overline{\mathbf{A}}^H\mathbf{R}_{\mathbf{x}}^{-1}\dot{\overline{\mathbf{A}}}_{a_n}\mathbf{R}_{\mathbf{s}}\overline{\mathbf{A}}^H\mathbf{R}_{\mathbf{x}}^{-1}\dot{\overline{\mathbf{A}}}_{\boldsymbol{\theta}}\}\\ &\quad+\mathrm{diag}\{\mathbf{R}_{\mathbf{s}}\overline{\mathbf{A}}^H\mathbf{R}_{\mathbf{x}}^{-1}\overline{\mathbf{A}}\mathbf{R}_{\mathbf{s}}\dot{\overline{\mathbf{A}}}_{a_n}^H\mathbf{R}_{\mathbf{x}}^{-1}\dot{\overline{\mathbf{A}}}_{\boldsymbol{\theta}}\}\}\end{aligned} \tag{B.17}$$

Similarly, other cross-terms can also be obtained.

B.4. The Cramer–Rao lower bound for DOA and mutual coupling

As the formulations we obtained above, we have

$$\begin{aligned}\mathbf{F}_{\boldsymbol{\theta a}} &= [\mathbf{F}_{\theta a_1},\ldots,\mathbf{F}_{\theta a_{P-1}}]\mathbf{F}_{\boldsymbol{a\theta}}\\ &= [\mathbf{F}_{a_1\theta}^T,\ldots,\mathbf{F}_{a_{P-1}\theta}^T]^T\mathbf{F}_{\boldsymbol{a}a}\\ &= \begin{bmatrix}\mathbf{F}_{a_1a_1} & \cdots & \mathbf{F}_{a_1a_{P-1}}\\ \vdots & \ddots & \vdots\\ \mathbf{F}_{a_{P-1}a_1} & \cdots & \mathbf{F}_{a_{P-1}a_{P-1}}\end{bmatrix}\end{aligned} \tag{B.18}$$

and the matrices $\mathbf{F}_{\boldsymbol{\theta b}}$, $\mathbf{F}_{\boldsymbol{\varphi a}}$, $\mathbf{F}_{\boldsymbol{\varphi b}}$, $\mathbf{F}_{\boldsymbol{a\varphi}}$, $\mathbf{F}_{\boldsymbol{b\theta}}$, $\mathbf{F}_{\boldsymbol{b\varphi}}$, $\mathbf{F}_{\boldsymbol{ba}}$, $\mathbf{F}_{\boldsymbol{ab}}$, $\mathbf{F}_{\boldsymbol{bb}}$ can be similarly obtained. Then the whole FIM can be given by the following expression:

$$\mathbf{F} = \begin{bmatrix}\mathbf{F}_{\boldsymbol{\theta\theta}} & \mathbf{F}_{\boldsymbol{\theta\varphi}} & \mathbf{F}_{\boldsymbol{\theta a}} & \mathbf{F}_{\boldsymbol{\theta b}}\\ \mathbf{F}_{\boldsymbol{\varphi\theta}} & \mathbf{F}_{\boldsymbol{\varphi\varphi}} & \mathbf{F}_{\boldsymbol{\varphi a}} & \mathbf{F}_{\boldsymbol{\varphi b}}\\ \mathbf{F}_{\boldsymbol{a\theta}} & \mathbf{F}_{\boldsymbol{a\varphi}} & \mathbf{F}_{\boldsymbol{a}a} & \mathbf{F}_{\boldsymbol{a}b}\\ \mathbf{F}_{\boldsymbol{b\theta}} & \mathbf{F}_{\boldsymbol{b\varphi}} & \mathbf{F}_{\boldsymbol{b}a} & \mathbf{F}_{\boldsymbol{b}b}\end{bmatrix} \tag{B.19}$$

Define $\mathbf{G} = \mathbf{F}^{-1}$, and consequently, we have the CRBs as follows:

$$CRB_{\boldsymbol{\Theta}} = \sqrt{\frac{1}{2K}\sum_{i=1}^{2K}\mathbf{G}_{ii}} \tag{B.20}$$

$$CRB_{\mathbf{c}} = \sqrt{\frac{1}{\|\mathbf{c}'\|^2}\sum_{i=2K+1}^{2K+2P-2}\mathbf{G}_{ii}}\times 100\% \tag{B.21}$$

where $CRB_{\boldsymbol{\Theta}}$ is the absolute CRB for DOA and $CRB_{\mathbf{c}}$ is the relative CRB for mutual coupling.

References

[1] R.O. Schmidt, Multiple emitter location and signal parameter estimation, IEEE Transaction on Antennas and Propagation 34 (3) (March 1986) 276–280.

[2] R. Roy, T. Kailath, ESPRIT-estimation of signal parameters via rotational invariance techniques, IEEE Transaction on Acoustics, Speech and Signal Processing 37 (7) (July 1989) 984–995.

[3] A.J. Weiss, B. Friedlander, Mutual coupling effects on phase-only direction finding, IEEE Transaction on Antennas and Propagation 40 (5) (May 1992) 535–541.

[4] T. Svantesson, The effects of mutual coupling using a linear array of thin dipoles of finite length, in: Ninth IEEE Signal Processing Workshop on Statistical Signal and Array Processing, September 1998, pp. 232–235.

[5] K.R. Dandekar, H. Ling, G. Xu, Effect of mutual coupling on direction finding in smart antenna applications, Electronics Letters 36 (22) (October 2000) 1889–1891.

[6] C.C. Yeh, M.L. Leou, D.R. Ucci, Bearing estimations with mutual coupling present, IEEE Transaction on Antennas and Propagation 37 (10) (October 1989) 1332–1335.
[7] B.C. Ng, C.M.S. See, Sensor-array calibration using a maximum-likelihood approach, IEEE Transaction on Antennas Propagation 44 (6) (June 1996) 827–835.
[8] C. Cheng, Y. Lv, A calibration algorithm for mutual coupling errors of array sensors based on the nonlinear constraint, in: The 2006 4th Asia-Pacific Conference on Environmental Electromagnetics, August 2006, pp. 486–489.
[9] T.T. Zhang, Y.L. Lu, H.T. Hui, Simultaneous estimation of mutual coupling matrix and DOAs for UCA and ULA, in: 17th International Zurich Symposium on Electromagnetic Compatibility, March 2006, pp. 265–268.
[10] B. Yu, C. Yin, Y. Huang, Calibration method for mutual coupling between elements based on parallel genetic algorithm, in: Proceedings of the 6th World Congress on Intelligent Control and Automation, 2006, pp. 3490–3493.
[11] B.K. Lau, J.B. Andersen, Direction-of-arrival estimation for closely coupled arrays with impedance matching, in: 6th International Conference on Information, Communications and Signal Processing, 2007, pp. 1–5.
[12] B. Friedlander, A.J. Weiss, Direction finding in the presence of mutual coupling, IEEE Transaction on Antennas and Propagation 39 (3) (March 1991) 273–284.
[13] F. Sellone, A. Serra, An iterative algorithm for the compensation of toeplitz mutual coupling in uniform and linear arrays, in: 12th Digital Signal Processing Workshop, September 2006, pp. 438–443.
[14] Y. Zhang, Q. Wan, A. Huang, W. Yang, Observation data based DOA estimation with uncalibrated antenna array in perspective of sparse solution finding, in: IEEE Region 10 Conference on TENCON, 2007, pp. 1–4.
[15] B. Wang, Y. Wang, H. Chen, A robust DOA estimation algorithm for uniform linear array in the presence of mutual coupling, in: IEEE Antennas and Propagation Society International Symposium, vol. 3, June 2003, pp. 924–927.
[16] M. Lin, L. Yang, Blind calibration and DOA estimation with uniform circular arrays in the presence of mutual coupling, IEEE Antennas and Wireless Propagation Letter 5 (1) (December 2006) 566–568.
[17] C. Qi, Z. Chen, Y. Zhang, Y. Wang, DOA estimation and self-calibration algorithm for multiple subarrays in the presence of mutual coupling, in: IET Proceeding and Radar Sonar and Navigation, vol. 153 (4), August 2006, pp. 333–337.
[18] Z. Ye, C. Liu, On the resiliency of MUSIC direction finding against antenna sensor coupling, IEEE Transactions on Antennas and Propagation 56 (2) (February 2008) 371–380.
[19] C. Liu, Z. Ye, Y. Zhang, DOA estimation based on fourth-order cumulants with unknown mutual coupling, Signal Processing 89 (9) (April 2009) 1839–1843.
[20] Z. Liu, Z. Huang, F. Wang, et al., DOA estimation with uniform linear arrays in the presence of mutual coupling via blind calibration, Signal Processing 89 (7) (February 2009) 1446–1456.
[21] R. Goossens, H. Rogier, A hybrid UCA-RARE/root-MUSIC approach for 2-D direction of arrival estimation in uniform circular arrays in the presence of mutual coupling, IEEE Transactions on Antennas and Propagation 55 (3) (March 2007) 841–849.
[22] Z. Ye, C. Liu, 2-D DOA estimation in the presence of mutual coupling, IEEE Transactions on Antennas and Propagation 56 (10) (October 2008) 3150–3158.
[23] M. Grice, J. Rodenkirch, et al., Direction of arrival estimation using advanced signal processing, in: 3rd International Conference on Recent Advances in Space Technologies, June 2007, pp. 515–522.
[24] S. Lundgren, A study of mutual coupling effects on the direction finding performance of ESPRIT with a linear microstrip patch array using the method of moments, in: International Symposium on Antennas and Propagation Society, vol. 2, July 1996, pp. 1372–1375.
[25] R. Klemm, Antenna design for adaptive airborne MTI, in: Radar 92. International Conference, October 1992, pp. 296–299.
[26] J.E. Fernandez del Rio, O.M. Conde-Portilla, M.F. Catedra, Estimating azimuth and elevation angles when mutual coupling is significant, in: Antennas and Propagation Society International Symposium, vol. 1, June 1998, pp. 215–218.
[27] Y.C. Yu, M. Okada, H. Yamamoto, Dummy elements add on both sides of monopole-array assisted doppler spread compensator for digital terrestrial television broadcasting receiver, in: IEEE International Workshop on Antenna Technology Small Antennas and Novel Metamaterials, March 2006, pp. 377–380.
[28] T. Svantesson, Modeling and estimation of mutual coupling in a uniform linear array of dipoles, in: Proceedings of the International Conference on Acoustics, Speech, and Signal Processing, vol. 5, March 1999, pp. 2961–2964.
[29] T. Svantesson, Mutual coupling compensation using subspace fitting, in: Proceedings of the IEEE Sensor Array and Multichannel Signal Processing Workshop, March 2000, pp. 494–498.
[30] M. Wax, T. Kailath, Detection of signals by information theoretic criteria, IEEE Transactions on Acoustics, Speech, Signal Processing 33 (2) (February 1985) 387–392.